Clays and Clay Minerals, Vol. 62, No. 2, 112–125, 2014.

THE TIMING OF DIAGENESIS AND THERMAL MATURATION OF THE CRETACEOUS MARIAS RIVER SHALE, DISTURBED BELT, MONTANA

Stephen G. Osborn[1,2], Louise Totten Duffield[3,5], W. Crawford Elliott[2,*], J. M. Wampler[2,4], R. Douglas Elmore[5], and Michael H. Engel[5]

[1] Department of Geological Sciences, California State Polytechnic University, Pomona, CA 91768, USA
[2] Department of Geosciences, Georgia State University, Atlanta, GA 30302-4105, USA
[3] Anadarko Petroleum Corporation, 1201 Lake Robbins Drive, The Woodlands, TX 77380, USA
[4] School of Earth and Atmospheric Sciences, Georgia Institute of Technology, Atlanta, GA 30332-0340, USA
[5] ConocoPhillips School of Geology and Geophysics, University of Oklahoma, Norman, OK 73019, USA

Abstract—The hypothesis that chemical remanent magnetization (CRM) in argillaceous rocks may be due to release of Fe during smectite illitization has been tested by study of spatial and temporal relationships of CRM acquisition, smectite illitization, and organic-matter maturation to deformation in the Montana Disturbed Belt. New K-Ar ages and stacking order and percentages of illite layers in illite-smectite (I-S) are consistent with conclusions from previous studies that smectite illitization of bentonites in Subbelts I and II of the Disturbed Belt was produced by thrust-sheet burial resulting from the Laramide Orogeny. Internally concordant, early Paleogene, K-Ar age values (55−57 Ma) were obtained from clay sub-fractions of thick bentonites which were significantly different in terms of their ages (*i.e.* Jurassic Ellis Formation and late Cretaceous Marias River Shale), further supporting a model of smectite illitization as a result of the Laramide Orogeny. Internally concordant K-Ar ages were found also for clay sub-fractions from a thick bentonite at Pishkun Canal (54 Ma) and from an undeformed bentonite near Vaughn on the Sweetgrass Arch (48 Ma). In Subbelts I and II, a greater degree of smectite illitization corresponds to increased thermal maturation, increased natural remanent magnetization intensity, and increased deformation (dip of beds). A dissolution−precipitation model over a short duration is proposed for the formation of illite layers in Subbelts I and II. A characteristic remanent magnetization was developed before or just after folding began in the early Paleogene. More smectite-rich I-S, low thermal maturity, and the absence of a CRM were noted in one outcrop of an undeformed rock on the Sweetgrass Arch. Strontium isotope data allow for the possibility that internal or externally derived fluids may have influenced illitization, but the K-Ar age values suggest that illitization was probably in response to conductive heating after the overthrusting had occurred. The differences in K-Ar dates among the bentonites studied herein may be due to differences in the timing of peak temperature related to differences in distance below the overthrust slab, in rates of burial and exhumation, and in initial temperature.

Key Words—Illite, K-Ar, Montana Disturbed Belt, Remagnetization, Thermal Maturity.

INTRODUCTION

A number of methods provide useful information about the thermal maturity of petroleum source rocks in sedimentary basins. These methods include the study of (1) diagenetic inorganic minerals (clays, oxides, carbonates), (2) organic geochemical parameters (vitrinite reflectance, time-temperature index, biomarkers), (3) the timing of diagenetic mineral transformations (from isotopic dating and remanent magnetization), (4) the geochemistry of basin brines, and (5) constructed burial curves and numerical models simulating burial temperatures. Knowledge of the timing of thermal maturation relative to that of the formation of suitable traps for crude oil and natural gas is critical for successful hydrocarbon exploration (Pevear, 1999).

* E-mail address of corresponding author:
wcelliott@gsu.edu
DOI: 10.1346/CCMN.2014.0620204

The degree of illitization of smectite, indicated by the type of stacking order and the percentage of illite layers in diagenetic mixed-layered illite-smectite (I-S), is well known as a gauge of thermal maturity in basins where conversion of smectite to illite (smectite illitization) was caused by burial, and the timing of the illitization can be determined by K-Ar dating (Hoffman *et al*., 1976; Hower *et al*., 1976; Hoffman and Hower, 1979; Elliott *et al*., 1991; Pollastro, 1994; Pevear, 1999; Clauer and Lerman, 2012; Stroker *et al*., 2013, Środoń *et al*., 2013). Smectite illitization also occurs in accretionary wedges, near igneous intrusions (by contact metamorphism or hydrothermal activity), and in other settings where the transformation is prompted by increases in temperature and potassium concentration (Aronson and Lee, 1986; Nadeau and Reynolds, 1981; Schoonmaker *et al*., 1986; Elliott and Matisoff, 1996; Bauluz *et al*., 2002; Kim and Peacor, 2002; Clauer, 2006; Derkowski *et al*., 2013). Externally derived fluids can cause diagenetic changes, particularly in mountain belts (Garven and Freeze, 1984; Oliver, 1986; Osborn *et al*., 2012). These external fluids

influence clay diagenesis in foreland basins adjacent to tectonic highlands (Morton, 1985; Elliott and Aronson, 1987; Elliott and Aronson, 1993; Ziegler and Longstaffe, 2000; Elliott and Haynes, 2002; Środoń *et al*., 2009). The conversion of smectite to illite proceeds either by solid-state transformation or dissolution-precipitation reactions; the latter mechanism prevails in fluid-dominated systems (Altaner and Ylagan, 1997).

The conversion of smectite to illite can release iron, which in turn precipitates as authigenic magnetite (Katz *et al*., 2000). Such authigenic magnetite can hold a measureable chemical remanent magnetization (CRM), the timing of which is relatable to the apparent polar wandering curve (Katz *et al*., 2000; Gill *et al*., 2002; Woods *et al*., 2002; Tohver *et al*., 2008; Elmore *et al*., 2012). Thus, a CRM can provide another basis for establishing the timing of diagenetic processes in argillaceous rocks, in particular where the timing of potassic diagenesis is difficult to determine in the clay fraction due to the presence of detrital I-S or detrital illite (Elliott *et al*., 2006a; Tohver *et al*., 2008; Zwing *et al*., 2009).

The Disturbed Belt in northwestern Montana is a good place to investigate the controls on clay diagenesis. The eastern and central parts of the Disturbed Belt consist of generally NW–SE trending folded and thrust-faulted Paleozoic and Mesozoic rocks. The last episode of disturbance was the late Cretaceous through early Paleogene Laramide Orogeny, which deformed Devonian–Cretaceous rocks (Mudge, 1982). To the east, the Disturbed Belt is bounded by gently folded Mesozoic rocks on the Sweetgrass Arch. Diagenesis in the Cretaceous rocks can be fit into a well known context of burial and thermal history. Clay-mineral thermometry was well established in an earlier study of the Disturbed Belt (Hoffman and Hower, 1979). Preliminary studies suggested that CRM in the Disturbed Belt Cretaceous rocks could be related to illitization, although other remagnetization mechanisms are possible (Gill *et al*., 2002; Elliott *et al*., 2006b).

I-S from Cretaceous shales and bentonites in the Disturbed Belt was studied by Hoffman and Hower (1979) and Hoffman *et al*. (1976) who found that ordered I-S with a high percentage of illite layers (>60% in most cases) was the most common clay mineral. Diagenetic illite formed in response to heating due to thrust sheet burial, according to Hoffman *et al*. (1976), and those authors used K-Ar ages of I-S to suggest that the thrusting had ended in the Paleocene. In almost undeformed stratigraphically equivalent units on the Sweetgrass Arch to the east, the clay fractions are dominated by randomly interstratified I-S with a high proportion of smectite layers (>70% in most cases), which indicates maximum burial temperatures of ~50ºC (Hoffman *et al*., 1976; Hoffman and Hower, 1979). The smectite-to-illite transformation in a 2.5 m-thick bentonite in the Sun River Canyon was studied by Altaner *et al*. (1984) who found that the percentage of illite layers and K-Ar ages of I-S decreased together from the edge (54 Ma) to the center (50 Ma) of this bentonite. These data were used to derive a model for diffusive transport of potassium and the formation of illite in thick bentonites (Altaner, 1989). The clay fractions of many samples collected from a ~2 m-thick bentonite from the Sun River Canyon (near Pishkun Canal) contained both R1 I-S and R0 I-S (McCarty *et al*., 2009). (The R descriptor is the Reichweite notation to denote the type of stacking order in I-S and other mixed-layered clay minerals; Jagodzinski, 1949; Moore and Reynolds, 1997). The center of this thick bentonite contained more R0 I-S and less R1 I-S than did the edges, but the percentage of illite layers in each of these kinds of I-S was the same throughout the bentonite. The I-S in this thick potassium bentonite was formed by simultaneous nucleation and growth according to Eberl *et al*. (2011). The diffraction patterns showing separate R1 I-S and R0 I-S (McCarty *et al*., 2009) can be explained as interparticle diffraction. The illite clay mineralogy of this thick potassium bentonite consists of continuous distributions of illite and smectite crystals (Eberl *et al*., 2011).

A temporal relationship between clay diagenesis and remagnetization was sought by Gill *et al*. (2002) who compared results from several different Mesozoic units in the Disturbed Belt with results from equivalent smectite-rich strata on the adjacent Sweetgrass Arch. The Disturbed Belt rocks contain a pre-folding or early syn-folding, reversed, Paleogene magnetization that is interpreted to be a CRM residing in magnetite and perhaps pyrrhotite. The rocks on the Sweetgrass Arch have weak magnetization and do not contain the CRM (Gill *et al*., 2002). A presence-absence test and the timing of acquisition of the CRM suggested that magnetite authigenesis could have been causally related to the conversion of smectite to illite. Support for such a relation was added by Elliott *et al*. (2006b) by finding that the timing of CRM acquisition in limestone concretions of the Cretaceous Marias River Shale is consistent with K-Ar ages of diagenetic illite from a thick (30 cm) bentonite near concretion beds. A late Jurassic to early Paleogene CRM that resides in magnetite in the Mississippian Madison Group carbonates of the Disturbed Belt was found by O'Brien *et al*. (2007). The CRM is pre-tilting in the thrust sheets and one anticline with a fault-bend geometry but syn-tilting in two fault-propagation folds. Petrographic and geochemical studies indicated that this CRM is related to evolved fluids that carried radiogenic Sr or to hydrocarbons (O'Brien *et al*., 2007).

Building on these past efforts, the present study was intended to test further the hypothesis that CRM acquisition in the Disturbed Belt was caused by smectite illitization, by more detailed investigation than before of how CRM acquisition, illitization, and organic

https://doi.org/10.1346/CCMN.2014.0620204 Published online by Cambridge University Press

maturation were spatially and temporally related to deformation in the Disturbed Belt. The Upper Cretaceous (Cenomanian to mid-Santonian), marine Marias River Shale, which overlies unconformably the lower Cretaceous Blackleaf Formation and consists predominantly of dark gray shale that is up to ~400 m thick. A few samples from the Blackleaf Formation and the Jurassic Ellis Formation were also investigated. Thus, some new K-Ar age values from bentonites (Jurassic Ellis Formation at Swift Dam, Cretaceous Marias River Shale at Badger Creek) and new paleomagnetic data from limestone concretions in the Marias River Shale (at Badger Creek) are presented and integrated with K-Ar and paleomagnetic data from Pishkun Canal (Elliott *et al*., 2006b) to further elucidate the remagnetization mechanism(s). These data are integrated with biomarker, geochemical, and clay mineralogical data to test the hypothesis regarding the origin of CRM in relation to smectite illization. These data further address the causes and timing of diagenesis and thermal maturation of Mesozoic rocks in the Disturbed Belt.

MATERIALS AND METHODS

Samples were collected from Subbelts I and II of the Disturbed Belt in Montana, which consists of Mesozoic strata that were deformed during the Laramide Orogeny (Mudge, 1982). Most samples were collected from the calcareous Cone Member of the Marias River Shale, which contains dark gray shale, limestone concretions, thin beds of limestone, and bentonites (Cobban *et al*., 1959). The Cone Member was probably a hydrocarbon source rock in the Disturbed Belt and is a known reservoir rock for crude oil and natural gas in the Sweetgrass Arch (Clayton *et al*., 1982). Samples were also collected from horizontal beds of the Vaughn Member of the Blackleaf Formation shale at the Sweetgrass Arch (Vaughn, Montana), and from a nearly overturned section of the Jurassic Ellis Formation at Swift Dam (Figure 1).

Concretions, bentonites, and carbonaceous shales were sampled at two outcrops (Badger Creek and Pishkun Canal) of the Marias River Shale and at one outcrop of the Blackleaf Formation at Vaughn (Figure 1). Results of studies of some of the collected samples, specifically K-Ar and clay mineral data from the Pishkun Canal bentonites and paleomagnetic data from one Pishkun Canal site and two Badger Creek sites, were published in a short, conference-related report (Elliott *et al*., 2006b). Limestone concretions are aligned with the direction of bedding and are from a few centimeters to ~30 cm in diameter. The bedding of the shale dips 75ºE at Pishkun Canal and from 20ºSW to 30ºSW at Badger Creek. Thick (>5 cm) bentonites were collected at both Badger Creek and Pishkun Canal. Thin

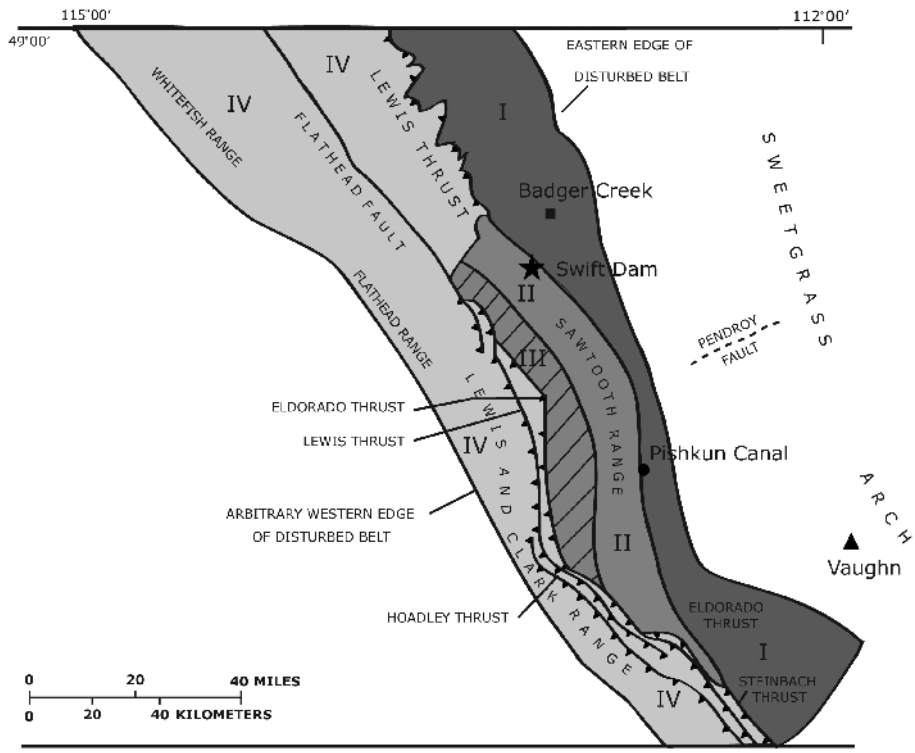

Figure 1. Map of the study area in Montana and sampling locations: Badger Creek (square), Swift Dam (star), Pishkun Canal (circle), and Vaughn (triangle). Areas I–IV refer to subbelts of the Disturbed Belt (modified from Mudge, 1982).

https://doi.org/10.1346/CCMN.2014.0620204 Published online by Cambridge University Press

bentonites (1–2 cm) were also collected at Badger Creek. A thick bentonite from the Ellis Formation was sampled at Swift Dam. Locations (latitude, longitude) for the Badger Creek, Pishkun Canal, and Swift Dam outcrops were given by Osborn (2006).

Portions (~25 g) of the collected bentonite samples were treated, using the methods of Jackson (1979), to remove carbonate cements, bulk organic matter, and Fe oxide cements. The treated portions were separated into sand, silt, and clay fractions by timed settling. The clay fractions were separated into sub-micrometer size fractions by centrifugation. The mineralogy of the clay fractions, the percentage of illite layers in I-S, and the stacking order of I-S were determined by X-ray diffractometry (XRD) of oriented clay following methods of Hower (1981) and Moore and Reynolds (1997). The K-Ar age values of clay fractions and clay sub-fractions were determined by procedures detailed by Osborn (2006). The LP-6 Bio interlaboratory standard was analyzed for potassium and radiogenic argon five times (Table 1). These results agree with accepted values (Odin *et al*., 1982).

Cores (2.5 cm diameter) were drilled from the limestone concretions and oriented with an inclinometer and a Brunton Compass. The cores were cut into standard specimens (2.2 cm long). Natural remanent magnetization (NRM) was measured with a 2G Enterprises cryogenic magnetometer with DC squids at the Paleomagnetic Laboratory of The University of Oklahoma. Most samples were processed through 19 steps of thermal demagnetization by heating in an SC Thermal Demagnetizer for 1 h. Selected samples were treated by alternating field demagnetization to 120 mT before undergoing thermal demagnetization. The demagnetization data were displayed on orthogonal projections (Zijderveld, 1967) and the components of the magnetization were determined by principal component analysis (Kirschvink, 1980) with mean angular deviations of 10º or less. The intensity of characteristic remanent magnetization (ChRM) for each specimen was calculated and mean site intensities were determined. Mean directions were calculated with Fisher (1953) statistics. Isothermal remanent magnetization (IRM) acquisition and thermal decay measurements were also performed to identify the magnetic minerals (Lowrie, 1990). A tilt test was performed on the results from Badger Creek and Pishkun Canal. The ChRM directions from beds tilted by different amounts are compared after incremental rotations that produce the same degree of relative 'untilting' of each bed. The incremental rotations range from zero for *in situ* bed orientation to 100% for the original horizontal bed orientation. If the best grouping of ChRM directions is for zero rotation, then the magnetization is considered post-tilting. If the best grouping is after rotation to the horizontal, the magnetization is considered pre-tilting. Otherwise the magnetization is considered syn-tilting.

Hand samples of carbonaceous shales were collected for organic geochemical analyses. Weathered surfaces were removed with a Dremel drill, and each sample was broken into smaller pieces, which were then ground to fine powder with a mortar and pestle. Organic matter was extracted from the powders in a Soxhlet apparatus with a mixture of dichloromethane and methanol. Most of the solvent was removed by evaporation under a stream of N_2 gas and hexane was added to each extract. The solutions then sat overnight at room temperature so the asphaltene fractions would precipitate. After removal of the asphaltene fractions by centrifugation, the remaining hexane-soluble components were separated into their respective saturated, aromatic, and heteroatomic compound (those containing N, S, or O) fractions by column chromatography. Details of the method were reported by Totten (2005). The procedure of West *et al*. (1990) was used to isolate the branched and cyclic alkanes from a portion of each saturated fraction. The methods reported by Totten (2005) were used to analyze the saturated fractions by gas chromatography and their sub-fractions of branched and cyclic alkanes by gas chromatography-mass spectrometry. The terpanes used to calculate thermal maturity ratios (Ts/Tm; Seifert and Moldowan, 1986) were as follows: 18α-30-norneohopane (C29Ts); 17α-30-norneohopane (C29Tm); 18α,21β-22,29,30-trisnorhopane (C27Ts); and 17α,21β-22,29,30-trisnorhopane (C27Tm). T_{max} values determined from Rock-Eval pyrolysis were used to calculate vitrinite reflectance values for the samples (Totten, 2005).

Strontium isotope analysis was done at the University of Texas-Austin according to the methods described by Gao *et al*. (1992). After fractionation corrections to $^{86}Sr/^{88}Sr = 0.1194$, the $^{87}Sr/^{86}Sr$ ratios were normalized relative to a mean observed value of 0.71014 for the ratio in SRM 987 (National Institute of Standards and Technology).

RESULTS

Clay mineralogy and K-Ar dating of I-S

The clay mineralogy and the K-Ar age values of the clay sub-fractions from seven samples, and of the clay fraction of four of those samples, were determined (Table 1). At Badger Creek, several bentonites of variable thickness were sampled. Samples BC-03, BC-05, and BC-06 are from thin (1–2 cm) bentonites. BC-01 is from a thick (>5 cm) bentonite. The rectorite-like ordering (R1) was found in I-S from both Pishkun Canal and Badger Creek (BC-01 and BC-06), as indicated by a superlattice peak at 26–28 Å in diffraction patterns of air-dried clay. On glycol saturation of the clay, this peak shifted to 29–30 Å. The percentage of illite layers in I-S is between 60 and 70% in the thick bentonite BC-01 and also in a thin bentonite (BC-06). Greater percentages of illite layers in I-S (>90%) and higher ordering (R3) were found in other

https://doi.org/10.1346/CCMN.2014.0620204 Published online by Cambridge University Press

Table 1. Bentonite clay mineralogy and K-Ar data.

Location, Sample	Clay mineralogy	K (% by mass)	^{40}Ar* (%)	^{40}Ar* (pmol g^{-1})	K-Ar age (Ma)
Badger Creek					
BC-01 (<0.25 μm)	I-S (60−70% I), kt	3.68±0.04	87	367±6	56.6±1.0
BC-01 (0.25−1.0 μm)	I-S (60−70% I), kt	3.71±0.04	89	375±4	57.4±0.9
BC-01 (0.25−1.0 μm)a		3.82±0.04	89	378±4	56.2±0.8
BC-01 (1−2 μm)	I-S (60−70% I), kt	3.75±0.04	88	368±4	55.8±0.8
BC-01 (1−2 μm)a		3.64±0.04	88	365±4	56.9±0.9
BC-03 (<0.25μm)	I-S (>90% I), kt	3.01±0.05	78	658±8	121.9±2.3
BC-03 (<0.25 μm)a		2.97±0.06	74	662±8	124.1±2.9
BC-03 (0.25−1.0 μm)	I-S (>90% I), kt	3.09±0.03	94	1008±11	178.9±2.6
BC-03 (0.25−1.0 μm)a		3.08±0.03	95	1004±11	179.1±2.6
BC-03 (1−2 μm)	I-S (>90% I), kt	2.47±0.03	95	1046±12	228.6±3.9
BC-03 (1−2 μm)a		2.42±0.02	95	1042±12	232.5±3.3
BC-03 (< 2 μm)	I-S (>90% I), kt	3.18±0.07	89	851±12	148.2±3.7
BC-05 (<0.25 μm	I-S (>90% I), kt	3.78±0.04	94	883±10	129.8±1.9
BC-05 (0.25−1.0 μm)	I-S (>90% I), kt	3.24±0.03	95	1193±14	200.9±2.9
BC-05 (1−2 μm)	I-S (>90% I), kt	3.34±0.03	95	1107±13	181.9±2.6
BC-06 (<0.25 μm)	I-S (70−80% I), kt	3.34 ±0.03	85	354±4	60.2±0.9
BC-06 (0.25−1.0 μm)	I-S (70−80% I), kt	3.09 ±0.03	87	340±5	62.3±1.1
BC-06 (1.0−2.0 μm)	I-S (60−70% I), kt	2.80 ±0.03	89	343±5	69.3±1.2
Pishkun Canal					
SR-04 (<0.25 μm)	I-S (70−80% I)	4.14±0.08	81	389±5	53.3±0.8
SR-04 (0.25−1.0 μm)	I-S (70−80% I), kt	4.15±0.08	92	390±4	53.3±1.1
SR-04 (1.0−2.0 μm)	I-S (70−80% I), kt	4.14±0.07	88	395±5	54.1±1.1
SR-04 (<2 μm)	I-S (70−80% I), kt	3.98±0.11	84	363±5	51.9±1.6
Swift Dam					
SD-03 (<0.25 μm)	I-S (70−80% I), kt	4.47±0.05	88	436±5	55.3±0.8
SD-03 (0.25−1.0 μm)	I-S (80−90% I), kt	3.65±0.04	88	362±6	56.2±1.0
SD-03 (1.0−2.0 μm)	I-S (80−90% I), kt	3.37±0.03	86	330±4	55.7±0.8
Vaughn					
VQ (<0.25 μm)	I-S (20−30% I)	0.89±0.02	60	79±1	50.6±1.2
VQ (0.25−1.0 μm)	I-S (20−30% I), kt	0.95±0.01	66	86±1	51.7±0.8
VQ (1.0−2.0 μm)	I-S (20−30% I), kt	1.04±0.01	65	95±1	51.8±0.9
VQ (<2 μm)	I-S (10−20% I), kt	1.18±0.02	54	100 ±2	48.3±1.2
LP6 (Biotite interlaboratory standard)					
		8.12±0.12	96	1943±30	132.9±2.7
		8.34±0.08	97	1935±22	129.1±1.9
		8.25±0.08	97	1921±22	129.4±1.9
		8.37±0.09	97	1918±22	127.5±1.9
		8.23±0.08	97	1943±22	131.2±1.9
Accepted (Odin *et al*., 1982)		8.33±0.03		1930	127.7±1.4

Notes: An 'a' after the size fraction denotes duplicate K-Ar determination.
Kaolinite is abbreviated to kt. ^{40}Ar* stands for radiogenic Ar. The error values are twice the estimated standard deviation (2σ) owing to random error. Pishkun Canal data from Elliott *et al*. (2006b).

thin bentonites (BC-03 and BC-05). Representative diffraction patterns of the glycol-solvated <0.25 μm clay fractions from thick bentonites (BC-01, Pishkun Canal, and Swift Dam) and from a thin bentonite at Vaughn are shown in Figure 2.

K-Ar age values were concordant at ~56−57 Ma for the clay sub-fractions of the thick bentonite (BC-01) but not for those of the thin bentonites at Badger Creek. The criterion for concordance used herein is that age values differ by no more than the sum of their error values (the 2σ error estimates). If the age values of the three sub-fractions are weighted equally, then the mean age value for BC-01 I-S is 56.6 Ma and the sample standard deviation is 0.23 Ma. The mean age value with 2σ

https://doi.org/10.1346/CCMN.2014.0620204 Published online by Cambridge University Press

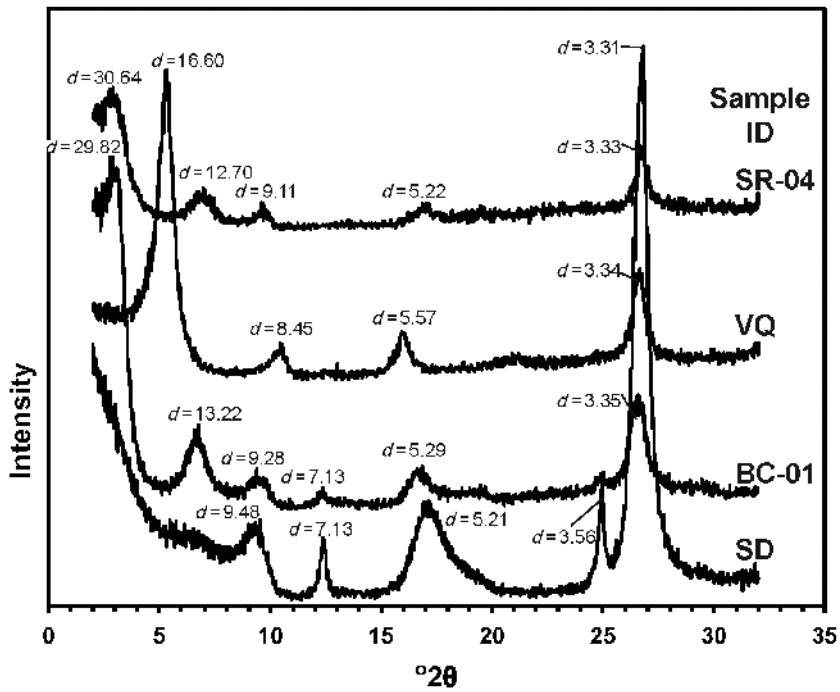

Figure 2. XRD patterns of the <0.25 μm fractions, glycol-solvated, of bentonites collected at Badger Creek (BC-01), Pishkun Canal (SR), Swift Dam (SD), and Vaughn (VQ). The *d* values are given in angstroms.

uncertainty is then 56.6 ± 0.5 Ma. For the BC-06 bentonite, the age values ranged from 60 to 69 Ma, but those of the two finer sub-fractions were concordant at 60−61 Ma.

Concordant K-Ar age values with a mean of 53.6 ± 0.9 Ma were determined for the clay sub-fractions of the bentonite from Pishkun Canal. This bentonite has more illite layers in I-S (70−80%) than the thick bentonite at Badger Creek (BC-01). I-S from the thick bentonite at Swift Dam has R3 stacking order and, in the two coarser clay sub-fractions, greater percentages of illite layers (>80%) than the Pishkun Canal bentonite. The K-Ar age values of clay sub-fractions of the Swift Dam bentonite were concordant with a mean of 55.7 ± 0.9 Ma. The percentage of illite layers in I-S from the bentonite sample collected near Vaughn is ~20% and the K-Ar ages of the clay sub-fractions were concordant with a mean of 51.4 ± 1.3 Ma.

Organic geochemical indicators of thermal maturity

The T_{max} values in the shale samples ranged from 431ºC to 457ºC (Table 2). The values were lower for shale from Badger Creek (431ºC and 433ºC) and Vaughn (437−439ºC) than for shale from Pishkun Canal (440−453ºC) and from the Ellis Formation at Swift Dam (445ºC and 452ºC). Values for vitrinite reflectance (R_o) calculated from the T_{max} values range from 0.6 at Badger Creek to near 1.0 at Pishkun Canal and Swift Dam (Table 2). The values for Vaughn were uncertain because of uncertainties in measuring the S2 peaks (Totten, 2005). The Badger Creek R_o values signify source rocks immature with respect to oil generation. The higher R_o values at Swift Dam and at Pishkun Canal signify thermal maturity within the oil-generating zone.

The ratios of selected biomarkers (C27 Ts/Tm, C29 Ts/Tm) were small for samples from Badger Creek and Vaughn. These ratios were much greater for samples from Swift Dam and Pishkun Canal (Figure 3, Table 2). These biomarker data are consistent with the T_{max} values observed for the shale samples at these localities.

Sr isotope ratios

The $^{87}Sr/^{86}Sr$ ratio observed for the concretion at Vaughn (0.7073) coincides with a coeval seawater value (0.7073−0.7074; McArthur *et al*., 2001; Mearon *et al*., 2003). The concretions at Badger Creek (0.7077) and Pishkin Canal (0.7081) had elevated values, greater than the coeval seawater value between 0.7073 and 0.7074.

Paleomagnetism

The measured NRM intensity in limestone concretions from the Marias River Shale ranged from 0.025 mA/m (Badger Creek) to 0.142 mA/m (Pishkun Canal). The magnetic intensities measured at Pishkun Canal were variable (0.074, 0.091, and 0.142 mA/m). The magnetic intensity found in a concretion from the Ellis Group at Swift Dam was 0.088 mA/m, and that found in two concretions from the Blackleaf Formation at Vaughan was 1.01 mA/m.

The demagnetization results revealed two components of the NRM, a viscous remanent magnetism (VRM) and a ChRM. At low temperatures (<~200ºC),

https://doi.org/10.1346/CCMN.2014.0620204 Published online by Cambridge University Press

Table 2. Biomarker, T_{max}, and NRM intensity data.

Location/ Sample	Ts/Tm C27	Ts/Tm C 29	CR	T_{max} (°C)	R_o	NRM (mA/m)
Badger Creek Concretion						0.025
04BC2	0.28	0.29	1.04	431	0.60	
04BC3	0.35	0.28	0.80	433	0.63	
Pishkun Canal Concretions						0.074, 0.091, 0.142
D11	4.45	1.18	0.27	450*	0.94*	
D10	4.21	1.26	0.30	453	0.99	
04 SR 6	5.78	1.44	0.25	452*	0.98*	
04 SR 5	7.11	1.75	0.25	440	0.76	
Swift Dam Concretion						0.088
04 SD 10	9.13	1.59	0.17	445*	0.85*	
04 SD 9A	5.44	0.76	0.14	452	0.98	
04 SD 9B	4.74	0.81	0.17	457*	1.07*	
Vaughn Concretions						0.101
04 VQ	0.27	0.26	0.96	439*	0.74*	
04 VQ 2	0.32	0.32	1.00	437*	0.71*	

Notes: CR = ratio of C29/C27. NRM = natural remanent magnetism. *The T_{max} and R_o derived from T_{max} should be viewed as estimated or approximate values based on S2 peak measurements (Totten, 2005; M. Engel, pers. comm.).

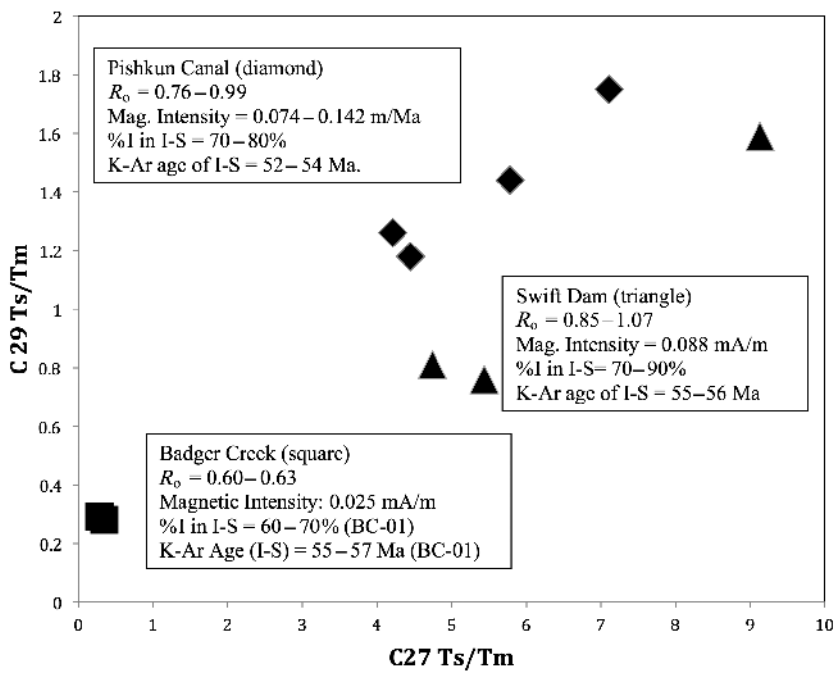

Figure 3. Plot of selected biomarker ratios (C27 Ts/Tm, C29 Ts/Tm) from Badger Creek (squares), Pishkun Canal (diamonds), and Swift Dam (triangles) from Totten (2005). NRM intensity, R_o, derived from T_{max} data, percentage of illite layers in I-S from thick bentonites, and range of concordant K-Ar age values are noted for each site.

https://doi.org/10.1346/CCMN.2014.0620204 Published online by Cambridge University Press

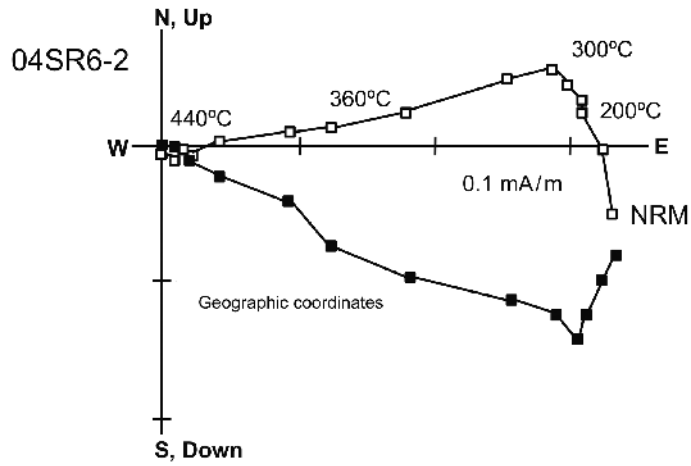

Figure 4. Representative Zijderveld diagram showing removal by thermal demagnetization of a modern VRM below 200ºC and of the ChRM between 200 and 440ºC. Open symbols: vertical component; closed symbols: horizontal component.

a northward and steeply downward component, interpreted to be a modern VRM, was removed from all concretion specimens. The ChRM from three Badger Creek limestone concretions and three Pishkun Canal limestone concretions, was removed between 200ºC and 440ºC (Figure 4). In geographic coordinates, the ChRM at the Pishkun Canal had east-southeasterly declinations and shallow inclinations whereas at Badger Creek the ChRM had southwesterly declinations and steeply upward inclinations (Figure 5; Table 3). The ChRMs were also removed by alternating field demagnetization from the Badger Creek and Pishkun canal specimens, which suggests the magnetization resided in a low-coercivity mineral such as magnetite or pyrrhotite. Most specimens from the concretions on the Sweetgrass Arch did not display stable decay. A few contained the modern VRM but did not display linear decay at unblocking temperatures above 250ºC.

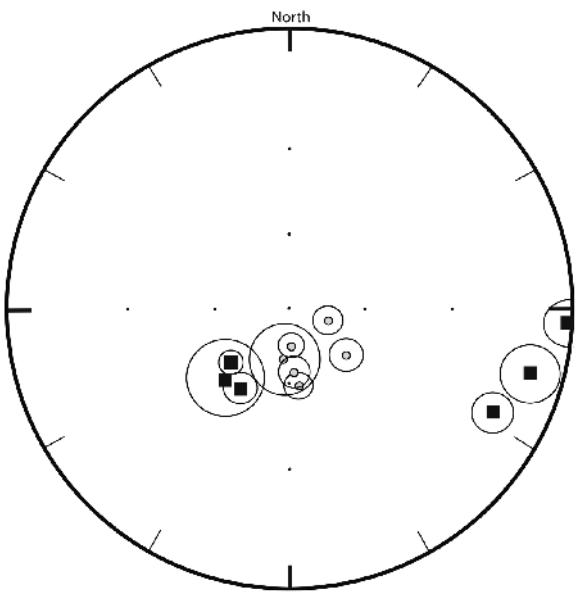

Figure 5. Equal area plot showing site mean directions with α95 circles in geographic (squares) and 100% tilt-corrected (small circles) coordinates. The best grouping is in tilt-corrected coordinates, which indicates magnetization before significant tilting occurred.

Assuming the ChRMs at Badger Creek and Pishkun Canal were contemporaneous, the mean site directions were used for a regional tilt test. Two results from two concretion sites at Pishkun Canal reported by Gill *et al.* (2002) were used in the tilt test. The site mean directions grouped best after correction for the tilt of the beds (100% untilting, declination = 160.2º, inclination = −69.1º, *k* [precision parameter] = 38.1, α95 [cone of 95% confidence] = 11.0º, *n* = 6; Figure 5). The Enkin (2003) tilt test indicates that the best grouping occurs at untilting of 114 ± 25%. The 95% confidence interval overlaps the 100% tilt correction and the ChRM could be interpreted as a pre-tilting magnetization. The 95% confidence interval is large, however, and the ChRM could also have been early syn-tilting.

The pole position for the 100% tilt-corrected direction is 185ºE, 77ºN (dp/dm [semi axes of 95% oval of confidence] = 15.9º/18.7º). This pole plots near the Paleogene part of the apparent polar wander path (Torsvik *et al.*, 2012). The directions for the ChRM were all reversed, which suggests that the ChRM is secondary, because the Marias River Shale was deposited during the Cretaceous Normal Polarity Superchron.

Magnetic intensity rose rapidly during IRM-acquisition studies of samples from Pishkun Canal (Gill *et al.*, 2002) and from Badger Creek (this study). Saturation was reached by 200−300 mT, suggesting that a low-coercivity phase dominates the magnetization. Thermal decay measurements of a triaxial IRM showed complete removal by 580ºC, indicating the presence of magnetite (Lowrie, 1990). A decrease in intensity of the low- and intermediate-coercivity components in the 300−320ºC

https://doi.org/10.1346/CCMN.2014.0620204 Published online by Cambridge University Press

Table 3. Site mean paleomagnetic data for carbonate concretions.

Locality	Site #	N/No	– *In situ* –		*k*	α95(º)	Tilt-corrected	
			Dec (º)	Inc (º)			Dec (º)	Inc (º)
Badger Creek	04BC2**	4/4	222.8	−52.7	44.6	13.9	186.4	−69.3
Badger Creek	04BC3**	8/9	212.1	−51.3	87.1	6.0	176.3	−63.9
Badger Creek	05BC4	9/9	227.4	−58.4	110.4	4.9	178.7	−74.9
Pishkun Canal	04SR6**	8/8	117.4	−11.7	131	4.9	173.4	−58.8
Pishkun Canal	D10*	6/7	105.4	6.7	100.1	6.7	129.1	−60.7
Pishkun Canal	D11*	9/9	92.9	0.4	108.8	5.0	108.7	−73.3

Notes: N/N_o – Number of specimens with direction *vs*. number of specimens demagnetized;
In situ – Geographic coordinate direction; Tilted – Stratigraphic coordinates; Dec – Declination;
Inc – Inclination; *k* – Precision parameter; α95 – Cone of 95% confidence.
* denotes data from Gill *et al*. (2002); ** denotes data published by Elliott *et al*. (2006b).

range also suggests the presence of pyrrhotite. These results suggest the ChRM in Disturbed Belt concretions found by stepwise demagnetization resides predominantly in magnetite. In contrast, the IRM-acquisition measurements of concretions from Vaughn showed an increase in intensity by 200 mT followed by a more gradual increase. These data suggest the presence of both lower- and higher-coercivity phases. Thermal-decay measurements showed removal of the low- and intermediate-coercivity curves by 580ºC. The high-coercivity curve was removed by 650−680ºC suggesting the presence of hematite.

INTERPRETATION AND DISCUSSION

Indicators of thermal maturity

The new clay-mineralogical results presented here are consistent with earlier work by Hoffman and Hower (1979) in that the I-S in bentonite samples from the Montana Disturbed Belt was ordered and illite-rich, while that in rocks on the Sweetgrass Arch I-S was randomly stacked and smectite-rich. The stacking order and percentage of illite layers in I-S suggest burial temperatures in the range 100−200ºC (Hoffman and Hower, 1979) for the Cretaceous rocks at Pishkun Canal and Badger Creek and for the Jurassic Ellis Formation from the same zone of the Disturbed Belt. Thus, the clay mineralogy indicates that these rocks were within the oil-generation window (Pevear, 1999). The new results are consistent with the previous interpretation that diagenetic illite formed in response to increased temperature due to thrust-sheet burial (Hoffman *et al*., 1976). The data from the present study indicate that the degree of smectite illitization in bentonite presently exposed in Subbelts I and II is variable. At the Badger Creek sampling site, farther north than the other Disturbed Belt sites and farther from the mountain front where the rocks were more intensely deformed, the percentage of illite layers found in I-S was 60−70%, less than at the other sites. The randomly ordered, smectite-rich I-S in bentonite from Vaughn denotes a much less thermally mature rock on the Sweetgrass Arch.

In addition to the evidence for clay diagenesis, the present study provides information from other indicators of thermal maturity. The Rock-Eval and biomarker results, including the calculated R_o values, indicate low thermal maturity of shale at the Badger Creek site and moderate thermal maturity at the two other Disturbed Belt sites. A difference of ~10% illite layers in I-S of bentonite coincides with a significant difference in thermal maturity of shale indicated by the Rock-Eval and biomarker data. The thermal maturity of Marias River Shale indicated by ratios of terpane compounds (Ts/Tm; Figure 3) is correlated with both percentage of illite layers in I-S and calculated vitrinite reflectance. In summary, a variety of indications of more active diagenesis correspond to increasing proximity to the mountain front and, thus, to increasing intensity of deformation in the Disturbed Belt.

K-Ar age values

The K-Ar age values for I-S from the thicker bentonites were <60 Ma and concordant across each set of clay sub-fractions. The larger and more variable age values for the clay sub-fractions of BC-06, from a thin Badger Creek bentonite, were probably due to small amounts of detrital illite – more in the coarse fraction than in finer ones – from shale originally entrained in the bentonite or included during collection of the bentonite. The predominance of detrital illite was indicated by much greater age values for BC-03 and BC-05 and also by >90% illite in the I-S.

The high degree of concordance of age values across the range of clay-particle size for each of the four thicker bentonites has several important implications. First, the concordance rules out a significant contribution of radiogenic argon by volcanogenic feldspar or mica (as well as by detrital minerals, already effectively ruled out

https://doi.org/10.1346/CCMN.2014.0620204 Published online by Cambridge University Press

by the thickness of the bentonite), because such minerals should be much older than the diagenetic I-S and relatively most abundant in the coarsest clay fraction. Second, the concordance rules out significant loss of radiogenic argon by thermal diffusion (proposed as significant under certain conditions by Clauer and Lerman, 2012), because such loss should have affected the finest I-S more than the coarser fractions. Third, the concordance indicates that the illite layers in I-S within each of the thicker illite-rich bentonites grew within a short time period, because thicker fundamental particles of illite are expected to be significantly younger than the thinnest ones if illitization occurred over an extended time period (Środoń *et al*., 2002). This inference does not apply to the poorly illitized bentonite from near Vaughn, because its illite fundamental particles, few in number relative to a larger number of smectite fundamental particles, should all be thin. This hypothesis can be tested through measuring particle-size distributions of the illitic clay fractions (Eberl *et al.*, 2011). Fourth, the concordance permits the time of illite formation within each sample to be better defined than it could be from a single K-Ar age determination, because concordant age values may be averaged with confidence to provide a mean age having less uncertainty than a single age value.

The age values of I-S from the thicker (>5 cm) bentonites (means of the concordant values from different clay sub-fractions) in the Disturbed Belt decrease southward, from 56.6 ± 0.5 Ma at Badger Creek, to 55.7 ± 0.9 Ma at Swift Dam, and to 53.6 ± 0.9 Ma at Pishkun Canal. The concordant age values for SR-04 at Pishkun Canal agree well with K-Ar age values of ~53–54 Ma reported by Altaner *et al*. (1984) for <1 μm size fractions of three samples of a 2.5 m thick bentonite in the Marias River Shale in the Sun River Canyon nearby. K-Ar data for clay fractions of two other bentonite samples from the Marias River Shale in the Sun River Canyon were also published by Hoffman *et al*. (1976); K-Ar age values for those two samples calculated from their radiogenic Ar and K_2O contents (with no adjustment for labile K) with the decay constants and isotopic abundances in current use (Steiger and Jäger, 1977) would be 51.4 Ma and 52.1 Ma (J.L. Aronson, pers. comm.). Thus, substantial evidence exists in support of illitization of smectite early in the Eocene Epoch in bentonites now exposed in the Sun River Valley. This illitization was notably later than the cessation of thrusting in the Disturbed Belt at ~59 Ma as inferred by Sears (2001). The data from the present study show a north-to-south progression of the effects of this thrusting. In particular, the similarity of K-Ar values of I-S from Jurassic and Cretaceous rocks supports a thrust-burial model for illitization.

The Pishkun Canal site is closer to the front ranges than the Badger Creek site. The rocks at Pishkun Canal are more strongly deformed. These rocks might have experienced deeper burial for a longer period of time as a result of thrust loading. Such prolonged thrust loading could have produced the younger illite at Pishkun Canal. If this interpretation is correct, then the timing of I-S formation may be explained by a dissolution-precipitation model (Altaner and Ylagan, 1997) in which radiogenic argon was released from older diagenetic illite as new and younger diagenetic illite was formed.

An alternative explanation of the younger illite at Piskun Canal might be found by seeking a mechanism for brief but later heating at Pishkun Canal than at Badger Creek and Swift Dam. The temporal temperature increase in footwall rock of major overthrusts in the Disturbed Belt was modeled by Hoffman and Hower (1979) who inferred that rocks within 200–300 m of a thick (6 or 7 km) overthrust sheet would have reached 'metamorphic temperatures' (>100ºC) soon (<1 m.y.) after the sheet was emplaced, owing to heat conduction downward. Those authors also inferred that under a thin overthrust sheet (~4 km), ~10 m.y. might be required for temperature to reach 100ºC, not from heat conducted downward but in response to restoration of a normal geothermal gradient in the rocks that had been buried by thrusting. From the then-available knowledge of thrust-sheet thicknesses, Hoffman and Hower (1979) inferred that rocks now exposed in the Sun River Canyon would have experienced the slower heating.

With respect to the differences in K-Ar age values, the thermal model of Hoffman and Hower (1979) offers an explanation – a slower heating in response to overthrusting – for the younger illite at Pishkun Canal than at Badger Creek and Swift Dam. That explanation, however, cannot account for the greater thermal maturity of the rocks at Pishkun Canal than at Badger Creek, evident from several indicators of thermal maturity applied in the present study. Furthermore, because Hoffman and Hower (1979) did not consider how denudation would have affected burial depth after emplacement of the thrust sheets, their model of slow heating of rock under thinner thrust sheets cannot account for the brief illitization implied by concordance of age values across the clay sub-fractions.

A detailed picture of the emplacement of a very thick thrust slab in the Montana Disturbed Belt during the Laramide Orogeny, including a description of the effects of the emplacement on the overridden footwall rocks was presented by Sears (2001). This picture included modeling of burial history in response to both the overthrusting and the subsequent rapid denudation (Sears, 2001, Figure 4). For rocks along the present-day mountain front, the model suggests rapid burial over 10–15 m.y. followed by somewhat more rapid exhumation over ~10 m.y. The model also implies that the maximum depth of thrust-slab burial (Sears, 2001, Figure 2), and consequently the rates of burial and subsequent exhumation, decreased rapidly toward the northeastern edge of the Disturbed Belt. The model of Sears (2001) provides a possible explanation for the

https://doi.org/10.1346/CCMN.2014.0620204 Published online by Cambridge University Press

strong but brief heating needed to account for a high degree of illitization in a short time period at Pishkun Canal and Swift Dam. For rock that had been more than ~⅓ km below the overriding slab, conductive heating after thrust-slab burial would have been due primarily to heat coming from hotter rock below, and the maximum temperature would have been reached substantially after deepest burial had occurred. That maximum temperature, the time elapsed before it was reached, and its effective duration would have depended on the initial temperature of the buried rock, on the maximum depth, and on the rates of burial and exhumation. Before deformation began, the Jurassic rock in the sedimentary column should have been warmer than the overlying Cretaceous rock; the difference in initial temperature perhaps accounts for the earlier illitization in the Jurassic bentonite at Swift Dam than in the Cretaceous rock to the south. The Sears (2001) model also suggests that the presently exposed rocks that are farther from the mountain front (Badger Creek) should have been closer to the overthrust slab, where they might have been heated promptly and briefly by heat moving downward from the thrust slab, but not as strongly over time as the then more deeply buried rocks now near the mountain front. If this idea is correct, then the K-Ar data indicate that thrust slab emplacement over what is now the Badger Creek area occurred at ~57 Ma. Such timing is not inconsistent with the inference of Sears (2001) that thrusting ended at ~59 Ma, because there could have been some systematic error in the K-Ar age values.

Fluids, either internal or externally derived, might also have influenced the timing and degree of illitization. Sears (2001) noted evidence that no metamorphic fluids were released from the overthrust slab, but he also described evidence for release of hot fluids from the more deeply buried footwall rocks and noted some likely effects of such fluids on rocks farther to the east. Insofar as release of fluids from deeply buried footwall rocks would have been driven by the immediate effect of increased pressure, rather than by the delayed effect of increased temperature, the effects of such fluids should have been manifest during the orogeny rather than after it ended. Such fluids moving eastward could have warmed sedimentary rocks above their initial temperature, however, thus influencing indirectly the timing of later illitization as well as causing geochemical changes in the rock. The results of the present study indicate that at least the concretions were altered by fluids with elevated $^{87}Sr/^{86}Sr$ ratios. This could mean that externally derived fluids altered the rocks. The dissolution of K-feldspar in shale by internal fluids generated by smectite illitization might also account for the elevated $^{87}Sr/^{86}Sr$ ratios.

In summary, concordant age values across clay subfractions of Disturbed Belt bentonites indicate that brief illitization occurred at about the time when thrusting ceased toward the north (Badger Creek and Swift Dam) and a few million years later toward the south (Sun River area). Post-thrusting heating of the overridden sedimentary rock owing to conductive heating could account for both the degree and timing of illitization, but this idea must remain hypothetical until much more relevant information is obtained. At this time, an effect of moving orogenic fluids on illitization of the bentonites remains a possibility.

Paleomagnetism

The burial temperatures in the Cretaceous rocks in the Disturbed Belt ranged from 100 to 200ºC according to estimates by Hoffman and Hower (1979). The calculated R_o values range from 0.60–0.63 at Badger Creek to 0.76–0.99 at Pishkun Canal. The maximum burial temperature was probably near 100ºC at Badger Creek but may have approached 200ºC at Pishkun Canal. If the maximum temperature was near 200ºC, the maximum unblocking temperature (440ºC) would have been too high for the ChRM to be a thermoviscous remanent magnetization (TVRM) caused by burial heating according to the time-temperature relationships of Pullaiah *et al*. (1975). The 200ºC estimate and the maximum unblocking temperatures, however, are consistent with a TVRM that resides partially in multidomain magnetite, based on other studies (*e.g.* Middleton and Schmidt, 1982; Kent, 1985). A maximum burial temperature of 100ºC, however, is probably too low for the ChRM to be thermoviscous in origin. Because the ChRM is present at Badger Creek, where burial temperatures were lower (maximum ~100ºC), the ChRM is interpreted as a CRM.

The presence of the CRM in the Disturbed Belt and its absence to the east suggests a genetic relation between the CRM and deformation of the Cretaceous rocks. The age based on pole position is not constrained well enough to make a precise comparison with the K-Ar illite ages. An early syn-tilting or pre-tilting CRM is not consistent with a connection between thrust loading and illitization, particularly considering the interpretation above that illitization at the Pishkun Canal site occurred several million years after cessation of thrusting. A pre-tilting CRM is problematic for a connection between thrust loading and the CRM. Pre-deformational burial depths for the Cretaceous rocks (<1 km) were too small to have caused illitization (*e.g.* Katz *et al.*, 2000) or maturation of organic matter (*e.g.* Banerjee *et al.*, 1997; Blumstein *et al.*, 2004) by burial alone. Several models for the origin of the CRM may be considered, including the migration of externally derived orogenic fluids (Oliver, 1992; Sears, 2001). One scenario is that the alteration could have been triggered by fluids that migrated in front of or were triggered to migrate by the deformation front to the west (*e.g.* Enkin *et al*., 2000; O'Brien *et al*., 2007). This scenario would be consistent with pre-tilting or syn-tilting CRM. The Sr isotope results, however, do not provide convincing evidence for

https://doi.org/10.1346/CCMN.2014.0620204 Published online by Cambridge University Press

alteration by external fluids because dissolution of K-feldspar in shale by internal fluids from smectite illitization could have generated the elevated $^{87}Sr/^{86}Sr$ ratios. The origin of the CRM in the concretions is unresolved, although it does provide evidence for a diagenetic event that caused acquisition of the CRM and precipitation of authigenic magnetite prior to or during early deformation.

The CRM reported in this study is similar to magnetizations from Paleozoic rocks in the southern Canadian Cordillera reported by Enkin *et al*. (2000) who noted a pre-folding Cretaceous CRM in magnetite, which was older in the west and younger in the east. Those authors proposed that the CRM was caused by alteration associated with a diagenetic front that moved eastward ahead of the deformation. They also reported the presence of a younger syn-tilting to post-tilting thermoviscous remagnetization in magnetite. A pre-tilting to early syn-tilting Early Cretaceous CRM in magnetite within folded Mississippian carbonate rocks in the southern Canadian Cordillera was reported by Zechmeister *et al*. (2102). Geochemical data and a vein-contact test suggested that the CRM was associated with fluids that migrated in front of the deformation front. They also reported an intermediate-temperature late syn-tilting to post-tilting CRM residing in pyrrhotite, which they attributed to thermal sulfate reduction.

SUMMARY

The clay mineralogy and the organic geochemistry data together provided a consistent view of the extent of thermal maturation as seen from the study of samples from three localities (Pishkun Canal, Badger Creek, and the Sweetgrass Arch). The concordant K-Ar data from the thick bentonites indicated that illite grew in a short time, perhaps *via* a dissolution-precipitation process. The K-Ar ages suggested some necessary revision of earlier ideas of how thrust burial prompted the formation of diagenetic illite in these bentonites. The thicknesses of bentonites were important for measuring concordant ages among these sub-fractions. The clay-mineral data (stacking order and percentage of illite layers) together with organic geochemistry data were consistent with the apparent extent of burial and deformation caused by thrust-sheet burial. The Sr geochemical data suggested that internal or externally derived fluids might have influenced illitization. Large percentages of illite layers were found with evolved organic matter, as indicated by calculated vitrinite reflectance values derived from T_{max} data and biomarker ratios, at Pishkun Canal (overturned beds). Smaller percentages of illite in I-S and less evolved organic matter were seen in moderately deformed strata at Badger Creek.

Although a broad genetic relationship is present among a CRM, thermal maturation, formation of diagenetic illite, and deformation in this study area, the K-Ar results of the present study did not support the hypothesis that acquisition of the CRM was caused by illitization. The paleomagnetic data provided evidence for a diagenetic event of unspecified origin prior to illitization that caused acquisition of a CRM residing in magnetite.

ACKNOWLEDGMENTS

This study comprised the Masters degree theses of Louise Totten at the University of Oklahoma and of Stephen G. Osborn at Georgia State University. The US Department of Energy Basic Energy Sciences provided funding for this study. The authors thank Venessa O'Brien and Shannon Dulin for help with sampling, John Zumberge and Kendra Imbus (GeoMark Research, Inc.) for their assistance with the biomarker data, and Dougal McCarty and an anonymous reviewer for their constructive comments.

REFERENCES

Altaner, S.P. (1989) Calculation of K diffusional rates in bentonite beds. *Geochimica et Cosmochimica Acta*, **53**, 923–931.

Altaner, S.P. and Ylagan, R.F. (1997) Comparison of structural models of mixed-layer illite/smectite and reaction mechanisms of smectite illitization. *Clays and Clay Minerals*, **45**, 517–533.

Altaner, S.P., Hower, J., Whitney, G., and Aronson, J.L. (1984) Model for K-bentonite formation: Evidence from zoned K-bentonites from the disturbed belt, Montana. *Geology*, **12**, 412–415.

Aronson, J.L. and Lee, M. (1986) K/Ar systematics of bentonite and shale in a contact metamorphic zone, Cerrillos, New Mexico. *Clays and Clay Minerals*, **34**, 483–487.

Banerjee, S., Elmore, R.D., and Engel, M.H. (1997) Chemical remagnetization and burial diagenesis; testing the hypothesis in the Pennsylvanian Belden Formation, Colorado. *Journal of Geophysical Research*, **102**, 24825–24842.

Bauluz, B., Peacor, D.R., and Ylagan, R.F. (2002) Transmission electron microscopy study of smectite illitization during hydrothermal alteration of a rhyolitic hyaloclastite from Ponza, Italy. *Clays and Clay Minerals*, **50**, 157–173.

Blumstein, A.M., Elmore, R.D., Engel, M.H., Elliot[*sic*], C., and Basu, A. (2004) Paleomagnetic dating of burial diagenesis in Mississippian carbonates, Utah. *Journal of Geophysical Research*, **109**, B04101. doi: 10.1029/2003JB002698.

Clauer, N. (2006) Towards an isotopic modeling of the illitization process based on data of illite-type fundamental particles from mixed-layer illite-smectite. *Clays and Clay Minerals*, **54**, 116–127.

Clauer, N. and Lerman, A. (2012) Thermal history analysis of sedimentary basins: An isotopic approach to illitization. Pp. 125–146 in: *Analyzing the Thermal History of Sedimentary Basins*: *Methods and Case Studies* (N.B. Harris and K.E. Peters, editors). SEPM Special Publication No. **103**, Society for Sedimentary Geology, Tulsa, Oklahoma, USA.

Clayton, J., Mudge, M.R., Sr., Lubeck, C., and Daws, T.A. (1982) Hydrocarbon source rock evaluation of the Disturbed Belt, northwestern Montana. Pp. 773–793 in: *Geologic Studies of the Cordilleran Thrust Belt, Volume II* (R.B. Powers, editor). Rocky Mountain Association of Geologists, Denver, Colorado, USA, **2**, p. 773–793.

Cobban, W.A., Erdmann, C.E., Lemke, R.W., and Manghen,

E.K. (1959) Revision of Colorado group on Sweetgrass arch, Montana. *AAPG Bulletin*, **43**, 2786–2796.

Derkowski, A., Bristow, T.F., Wampler, J.M., Środoń, J., Marynowski, L., Elliott, W.C., and Chamberlin, C.P. (2013) Hydrothermal alteration of the Ediacaran Doushantuo Formation in the Yangtze Gorges area (South China). *Geochimica et Cosmochimica Acta*, **107**, 279–298.

Eberl, D.D., Blum A.E., and Serravezza, M. (2011) Anatomy of a metabentonite: Nucleation and growth of illite crystals and their coalescence into mixed-layer illite/smectite. *American Mineralogist*, **96**, 586–593.

Elliott, W.C. and Aronson, J.L. (1987) Alleghanian episode of K–bentonite illitization in the southern Appalachian Basin. *Geology*, **15**, 735–739.

Elliott, W.C. and Aronson, J.L. (1993) The timing and extent of illite formation in Ordovician K-bentonites at the Cincinnati Arch, the Nashville Dome and north-eastern Illinois Basin. *Basin Research*, **5**, 125–135.

Elliott, W.C. and Haynes, J.T. (2002) The chemical character of fluids forming diagenetic illite in the Southern Appalachian Basin. *American Mineralogist*, **87**, 1519–1527.

Elliott, W.C. and Matisoff, G. (1996) Evaluation of kinetic models for the smectite to illite transformation. *Clays and Clay Minerals*, **44**, 77–87.

Elliott, W.C., Aronson, J.L., Matisoff, G., and Gautier, D.L. (1991) Kinetics of the smectite to illite transformation in the Denver Basin: clay mineral, K-Ar data, and mathematical model results. *The American Association of Petroleum Geologists Bulletin*, **75**, 436–462.

Elliott, W.C., Basu, A., Wampler, J.M., Elmore, R.D., and Grathoff, G.H. (2006a) Comparison of K-Ar ages of diagenetic illite-smectite to the age of a chemical remanent magnetization (CRM): An example from the Isle of Skye, Scotland. *Clays and Clay Minerals*, **54**, 314–323.

Elliott, W.C., Osborn, S.G., O'Brien, V.J., Elmore, R.D., Engel, M.H., and Wampler, J.M. (2006b) On the timing and causes of illite formation and remagnetization in the Cretaceous Marias River Shale, Disturbed Belt, Montana. *Journal of Geochemical Exploration*, **89**, 92–95.

Elmore, R.D., Muxworthy, A.R., and Aldana, M. (2012) Remagnetization and chemical alteration of sedimentary rocks. Pp. 1–21 in: *Remagnetization and Chemical Alteration of Sedimentary Rocks* (R.D. Elmore, A.R. Muxworthy, M.M. Aldana, and M. Mena, editors). Special Publications, **371**. Geological Society, London, doi:10.1144/SP371.15

Enkin, R.J. (2003) The direction-correction tilt test; an all-purpose tilt/fold test for paleomagnetic studies. *Earth and Planetary Science Letters*, **212**, 151–166.

Enkin, R.J., Osadetz, K.G., Baker, J., and Kisilevsky. D. (2000) Orogenic remagnetizations in the Front Ranges and Inner Foothills of the southern Canadian Cordillera: Chemical harbinger and thermal handmaiden of Cordilleran deformation. *Geological Society of America Bulletin*, **112**, 929–942.

Fisher, R. (1953) Dispersion on a sphere. *Proceedings of the Royal Society of London, Series A, Mathematical and Physical Sciences*, **217**, 295–305.

Gao, G., Elmore, R.D., and Land, L.S. (1992) Geochemical constraints on the origin of calcite veins and associated limestone alteration, Ordovician Viola Group, Arbuckle Mountains, Oklahoma, U.S.A. *Chemical Geology*, **98**, 257–269.

Garven, G. and Freeze, R.A. (1984) Theoretical analysis of the role of groundwater flow in the genesis of stratabound ore deposits. 1. Mathematical and numerical model. *American Journal of Science*, **284**, 1085–1124.

Gill, J.D., Elmore, R.D., and Engel, M.H. (2002) Chemical remagnetization and clay diagenesis: testing the hypothesis in the Cretaceous sedimentary rocks of northwestern Montana. *Physics and Chemistry of the Earth*, **27**, 1131–1139.

Hoffman, J. and Hower, J. (1979) Clay mineral assemblages as low grade metamorphic geothermometers: application to the thrust faulted disturbed belt of Montana, U.S.A. Pp. 55–79 in: *Aspects of Diagenesis* (P.A. Scholle and P.R. Schluger, editors). Society of Economic Paleontologists and Mineralogists, Special Publication **26**.

Hoffman, J., Hower, J., and Aronson, J.L. (1976) Radiometric dating of time of thrusting in the disturbed belt of Montana. *Geology*, **4**, 16–20.

Hower, J.F. (1981) X-ray diffraction of mixed layered clay minerals. Pp. 39–59 in: *Clays and the Resource Geologist* (F.J. Longstaffe, editor). Short Course **7**, Mineralogical Society of Canada.

Hower, J., Eslinger, E.V., Hower, M.E., and Perry, E.A. (1976) Mechanism of burial metamorphism of argillaceous sediment: 1. Mineralogical and chemical evidence. *Geological Society of America Bulletin*, **87**, 725–737.

Jackson, M.L. (1979) *Soil Chemical Analyses – Advanced Course*, second edition. Published by the author, Madison, Wisconsin, USA, 895 pp.

Jagodzinski, H. (1949) Eindimensionale Fehlordnung in Kristallen und ihr Einfluss auf die Röntgeninterferenzen. I. Berechnung des Fehlordnungsgrades aus den Röntgenintensitäten. *Acta Crystallographica*, **2**, 201–207.

Katz, B., Elmore, R.D., Cogoini, M., Engel, M.H., and Ferry, S. (2000) Associations between burial diagenesis of smectite, chemical remagnetization, and magnetite authigenesis in the Vocontian trough, SE France. *Journal of Geophysical Research*, **105(B1)**, 851–868.

Kent, D.V. (1985) Thermoviscous remagnetization in some Appalachian limestones. *Geophysical Research Letters*, **12**, 805–808.

Kim, J.-W. and Peacor, D.R. (2002) Crystal-size distributions of clays during episodic diagenesis: the Salton Sea Geothermal System. *Clays and Clay Minerals*, **50**, 371–380.

Kirschvink, J.L. (1980) The least-squares line and plane and the analysis of palaeomagnetic data. *Geophysical Journal of the Royal Astronomical Society*, **62**, 699–718.

Lowrie, W. (1990), Identification of ferromagnetic minerals in a rock by coercivity and unblocking temperature properties. *Geophysical Research Letters*, **17**, 159–162.

McArthur, J.M., Howarth, R.J., and Bailey, T.R. (2001) Strontium isotope stratigraphy: LOWESS version 3: Best fit to the marine Sr-isotope curve for 0–509 Ma and accompanying look-up table for deriving numerical age. *The Journal of Geology*, **109**, 155–170.

McCarty, D.K., Sakharov, B.A., and Drits, V.A. (2009) New insights into smectite illitization: A zoned K-bentonite revisited. *American Mineralogist*, **94**, 1653–1671.

Mearon, S., Paytan, A., and Bralower, T.J. (2003) Cretaceous strontium isotope stratigraphy using marine barite. *Geology*, **31**, 15–18.

Middleton, M.F. and Schmidt, P.W. (1982) Paleothermometry of the Sydney Basin. *Journal of Geophysical Research*, **87**, 5351–5359.

Moore, D.M. and Reynolds, R.C., Jr. (1997) *X-ray Diffraction and the Identification and Analysis of Clay Minerals*, second edition. Oxford University Press, New York, 378 pp.

Morton, J.P. (1985) Rb-Sr dating of diagenesis and source age of clays in Upper Devonian black shales of Texas. *Geological Society of America Bulletin*, **96**, 1043–1049.

Mudge, M.R. (1982) A resume of the structural geology of the Northern Disturbed Belt, northwestern Montana. Pp. 91–122 in: *Geologic Studies of the Cordilleran Thrust Belt, Volume I* (R.B. Powers, editor), Rocky Mountain Association of Geologists, Denver, Colorado, USA.

Nadeau, P.H. and Reynolds, R.C., Jr. (1981) Burial and contact metamorphism in the Mancos Shale: *Clays and Clay Minerals*, **29**, 249–259.

O'Brien, V.J., Moreland, K.M., Elmore, R.D., Engel, M.H., and Evans, M.A. (2007), Origin of orogenic remagnetizations in Mississippian carbonates, Sawtooth Range, Montana. *Journal of Geophysical Research*, **112**, B06103, doi:10.1029/2006JB004699.

Odin, G. and 35 collaborators (1982) Interlaboratory standards for dating purposes. Pp. 123–149 in: *Numerical Dating in Stratigraphy* (G.S. Odin, editor). John Wiley and Sons, New York.

Oliver, J. (1986) Fluids expelled tectonically from orogenic belts: Their role in hydrocarbon migration and other geologic phenomena. *Geology*, **14**, 99–102.

Oliver, J. (1992) The spots and stains of plate tectonics. *Earth-Science Reviews*, **32**, 77–106.

Osborn, S.G. (2006) The timing and causes of illite formation in the Cretaceous Marias River Shale, Disturbed Belt, Montana. M.S. Thesis, Georgia State University, Atlanta, Georgia, USA, 117 pp.

Osborn, S.G., McIntosh, J.C., Hanor, J.S., and Biddulph, D. (2012) Iodine-129, $^{87}Sr/^{86}Sr$, and trace elemental geochemistry of northern Appalachian Basin brines: Evidence for basinal-scale fluid migration and clay mineral diagenesis. *American Journal of Science*, **312**, 263–287, doi: 10.2475/03.2012.01

Pevear, D.R. (1999) Illite and hydrocarbon exploration. *Proceedings of the National Academy of Sciences*, **96**, 3440–3446.

Pollastro, R.M., (1994) Considerations and applications of the illite/smectite geothermometer in hydrocarbon-bearing rocks of Miocene to Mississippian age: *Clays and Clay Minerals*, **41**, 119– 133.

Pullaiah, G., Irving, E., Buchan, K.L., and Dunlop, D.J. (1975) Magnetization changes caused by burial and uplift. *Earth and Planetary Science Letters*, **28**, 133–143.

Schoonmaker, J., Mackenzie, F.T., and Speed, R.C. (1986) Tectonic implications of illite/smectite diagenesis, Barbados accretionary prism. *Clays and Clay Minerals*. **34**, 465–472.

Sears, J.W. (2001) Emplacement and denudation history of the Lewis-Eldorado-Hoadley thrust slab in the northern Montana Cordillera, USA: Implications for steady-state orogenic processes. *American Journal of Science*, **301**, 359–373.

Seifert, W.K. and Moldowan, J.M. (1986) Use of biological markers in petroleum exploration. Pp. 261–290 in: *Biological Markers in the Sedimentary Record* (R.B. Johns, editor). Methods in Geochemistry and Geophysics, **24**, Elsevier, Amsterdam.

Środoń, J., Clauer, N., and Eberl, D.D. (2002) Interpretation of K-Ar dates of illitic clays from sedimentary rocks aided by modeling. *American Mineralogist*, **87**, 1528–1535.

Środoń, J., Clauer, N., Huff, W., Dudek, T., and Banaś, M. (2009) K-Ar dating of the Lower Palaeozoic K-bentonites from the Baltic Basin and the Baltic Shield: implications for the role of temperature and time in the illitization of smectite. *Clay Minerals*, **44**, 361–387.

Środoń, J., Paszkowski, M., Drygant, D., Anczkiewicz, A., and Bana M. (2013) Thermal history of Lower Paleozoic rocks on the Peri-Tornquist margin of the East European Craton (Podolia, Ukraine) inferred from combined XRD, K-Ar, and AFT data. *Clays and Clay Minerals*, **61**, 107–132.

Steiger, R.H. and Jäger, E. (1977) Subcommission on Geochronology: Convention on the use of decay constants in geo- and cosmochronology. *Earth and Planetary Science Letters*, **36**, 359–362.

Stroker, T.M., Harris, N.B., Elliott, W.C., and Wampler, J.M. (2013) Diagenesis of a tight gas sand reservoir: Upper Cretaceous Mesaverde Group, Piceance Basin, Colorado. *Marine and Petroleum Geology*, **40**, 48–68.

Torsvik, T.H., Van der Voo, R., Preeden, U., Mac Niocaill, C., Steinberger, B., Doubrovine, P.V., van Hinsbergen, D.J.J., Domeier, M., Gaina, C., Tohver, E., Meert, J.G., McCausland, P.J.A., and Cocks, L.R.M. (2012) Phanerozoic polar wander, palaeogeography and dynamics. *Earth-Science Reviews*, **114**, 325–368.

Totten, L.A. (2005) Geochemical and paleomagnetic assessments of organic-rich lithologies in the disturbed belt, Montana. M.S. thesis, Oklahoma University, Norman, Oklahoma, USA, 79 pp.

Tohver, E., Weil, A.B., Solum, J.G., and Hall, C.M. (2008) Direct dating of carbonate remagnetization by $^{40}Ar/^{39}Ar$ analysis of the smectite–illite transformation. *Earth and Planetary Science Letters*, **274**, 524–530.

West, N., Alexander, R., and Kagi, R.I. (1990) The use of silicalite for rapid isolation of branched and cyclic alkane fractions of petroleum. *Organic Geochemistry*, **15**, 499–501.

Woods, S., Elmore, R.D., and Engel, M. (2002) Paleomagnetic dating of the smectite-to-illite conversion: testing the hypothesis in Jurassic sedimentary rocks, Skye, Scotland. *Journal of Geophysical Research*, **107**, 10.1029/2000JB000053, EPM 2-1-2-12.

Zechmeister, M.S., Pannalal, S., and Elmore, R.D. (2012) A multidisciplinary investigation of multiple remagnetizations within the Southern Canadian Cordillera, SW Alberta and SE British Columbia. Pp. 123–144 in: *Remagnetization and Chemical Alteration of Sedimentary Rocks* (R.D. Elmore, A.R. Muxworthy, M.M. Aldana, and M. Mena, editors). Special Publications, **371**. Geological Society, London, doi:10.1144/SP371.11.

Ziegler, K. and Longstaffe, F.J. (2000) Multiple episodes of clay alteration at the Precambrian/Paleozoic unconformity, Applachian Basin: Isotopic evidence for long-distance and local fluid migrations. *Clays and Clay Minerals*, **48**, 474–493.

Zijderveld, J.D.A. (1967) A.C. demagnetization of rocks – analysis of results. Pp. 254–286 in: *Methods in Paleomagnetism* (D.W. Collinson, K.M. Creer, and S.K. Runcorn, editors). *Developments in Solid Earth Geophysics*, **3**. Elsevier, Amsterdam.

Zwing, A., Clauer, N., Liewig, N., and Bachtadse, V. (2009) Identification of remagnetization processes in Paleozoic sedimentary rocks of the northeast Rhenish Massif in Germany by K-Ar dating and REE tracing of authigenic illite and Fe oxides. *Journal of Geophysical Research*, **114**, B06104 http://dx.doi.org/10.1029/2008JB006137

(*Received 16 January 2014; revised 26 May 2014; Ms. 836; AE: R.J. Pruett*)